



# A Study Of MHD Flow Of Casson Fluid Over An Exponentially Stretching Sheet With Heat Transfer.

Shamasuddin Wani<sup>1\*</sup>, Prof. R.K. Shrivastav<sup>2</sup>

<sup>1</sup>Ph.D. (Mathematics) Research Scholar, Email: sdinwani@gmail.com

<sup>2</sup>Professor and head of the department of mathematics at Agra College Agra. U.P, Email: dr.srivastavark@gmail.com

**\*Corresponding Author:** - Shamasuddin Wani

\*Ph.D. (Mathematics) Research Scholar, Email: sdinwani@gmail.com

In this paper, the problem of steady laminar two-dimensional boundary layer flow and heat transfer of MHD flow of Casson fluid with a presence of thermal radiation over an exponentially stretching sheet is investigated numerically. The governing boundary layer equations are reduced into ordinary differential equations using similarity transformation. The transformed equations are then solved numerically using Keller-box method. Numerical results are obtained for the velocity, temperature, skin friction coefficient and Nusselt number. The influence of the various governing parameters viz. Casson parameter, magnetic parameter, porosity parameter and Prandtl number on the flow and heat transfer characteristics of the Casson fluid is plotted graphically and discussed in detail.

**Keywords:** Boundary Layer Flow, Exponentially Stretching Sheet, Numerically Solution, Thermal Radiation

## 1. Introduction

The study of flow over a stretching sheet has generated tremendous interest in recent times, it is an important area of research undergoing rapid growth in viscous and non-Newtonian fluids. This is attracted by the investigators in view of their wide range of industrial applications such as the aerodynamic extrusion of plastic sheets, the boundary layer along a liquid film, condensation process of metallic plate in a cooling bath and glass, and also in polymer industries. Especially, the boundary layer flows in presence of magnetic field and heat transfer rate have pivotal role in the metallurgical process including cooling of continuous strips and filaments drawn through a quiescent fluid and the purification of molten metals from non-metallic inclusions. The quality of final product greatly depends upon the cooling rate in the manufacturing process. Such rate of cooling can be controlled by drawing the strips in MHD fluid, so that final product of the desired quality can be obtained. Cooling of nuclear reactors, liquid metal fluids, high-temperature plasmas, power generation systems are few applications of radiative heat transfer from a vertical wall to conductive gray fluids. Extensive excellent theoretical attempts under various aspects are presented regarding the boundary layer flows since the earliest study by Sakiadis (Sakiadis 1961). Here, we only refer few contributions on the topic (Yao et al. 2011; Fang et al. 2010; Ahmad and Asghar 2011; Rashidi et al. 2011; Hayat and Qasim 2010; Hayat et al. 2011a, b; Domairry and Ziabakhsh 2012; Bhattacharyya and Layek 2011).

It is worth mentioning that the studies of thermal radiation and heat transfer are important in electrical power generation, astrophysical flows, solar power technology and other industrial areas. A lot of extensive literature that deals with flows in the presence of radiation effects is now available. Elbashbeshy and Dimian (2002) analysed boundary layer flow in the presence of radiation effect and heat transfer over the wedge with viscous coefficient. Besides that, Cortell (2008) has solved a problem on the effect of radiation on Blasius flow by using fourth-order Runge-Kutta approach. Later, Sajid and Hayat (2008) considered the influence of thermal radiation on the boundary layer flow due to an exponentially stretching sheet by solving the problem analytically via homotopy analysis method (HAM). Recently, El-Aziz (2009) and Ishak (2009) also focused on the effects of thermal radiation in their studies.

In this paper, we investigate numerically the effect of thermal radiation on the steady laminar two-dimensional boundary layer flow and heat transfer over an exponentially stretching sheet, which has been solved analytically by Sajid and Hayat (2008). By employing the similarity transformation, the boundary layer equations are solved numerically using an efficient implicit finite-difference scheme known as the Keller-box method (Cebeci & Bradshaw, 1977, 1988).

## 2. Mathematical Formulation

Consider the two-dimensional flow of an incompressible viscous fluid bounded by a stretching sheet in which the x-axis is taken along the stretching sheet in the direction of the motion and y-axis is perpendicular to it. Under the usual boundary layer approximations, the flow and heat transfer in the presence of radiation effects are governed by the following equations (Sajid & Hayat, 2008):

$$\frac{\partial u}{\partial x} + \frac{\partial v}{\partial y} = 0 \tag{1}$$

$$u \frac{\partial u}{\partial x} + v \frac{\partial u}{\partial y} = \nu \left( \frac{\partial^2 u}{\partial y^2} \right) \tag{2}$$

$$\rho c_p \left( u \frac{\partial T}{\partial x} + v \frac{\partial T}{\partial y} \right) = k \left( \frac{\partial^2 T}{\partial y^2} \right) + u \left( \frac{\partial u}{\partial y} \right)^2 - \frac{\partial q_r}{\partial y}, \tag{3}$$

Where  $u$  and  $v$  are the velocities in the  $x$ - and  $y$ - directions respectively,  $\rho$  is the fluid density,  $\nu (= \mu/\rho)$  is the kinematic viscosity,  $\mu$  is the dynamic viscosity,  $T$  is the temperature,  $k$  is the thermal conductivity,  $c_p$  is the specific heat and  $q_r$  is the radiative heat flux. The boundary conditions are given by

$$u(0) = U_0 e^{\frac{x}{L}}, \quad v(0) = 0, \quad \frac{\partial T}{\partial y} = Bx^2 \quad \text{at } y = 0 \tag{4}$$

$$u \rightarrow 0, \quad T \rightarrow T_\infty \quad \text{as } y \rightarrow \infty$$

Where  $U_0$  is the reference velocity,  $b > 0$  is the stretching sheet velocity and  $T_\infty$  is the temperature far away from the plate while  $L$  is a constant.  $\ell$  is the characteristic length,  $T$  is the temperature of the fluid,  $k$  is the thermal conductivity,  $q_r$  is the radiative heat flux,  $C_p$  is the specific heat at constant pressure. The radiative heat flux can be written as

$$q_r = - \frac{4\sigma^* \partial T^4}{3k_1 \partial y}, \tag{5}$$

where  $k_1$  is the mean absorption coefficient and  $\sigma^*$  is the Stefan Boltzmann constant.  $T^4$  is expressed as a linear function of temperature, therefore

$$T^4 = 4T_\infty^3 T - 3T_\infty^4 \tag{6}$$

By using equations (3), (5) and (6) we can write as:

$$\rho c_p \left( u \frac{\partial T}{\partial x} + v \frac{\partial T}{\partial y} \right) = \left( k + \frac{16\sigma^* T_\infty^3}{3k_1} \right) \frac{\partial^2 T}{\partial y^2} + \mu \left( \frac{\partial u}{\partial y} \right)^2 \tag{7}$$

Introduce the following similarity transformations:

$$u = U_0 e^{x/L} f'(\eta), \quad v = \sqrt{\frac{\nu U_0}{2L}} e^{x/2L} \{ f(\eta) + \eta f'(\eta) \}, \quad T = T_0 e^{x/2L} \theta(\eta), \quad \eta = \sqrt{\frac{U_0}{2\nu L}} e^{x/2L} y. \tag{8}$$

Equation (1) is satisfied automatically and equations (2) and (7) are reduced as:

$$f''' - 2f'^2 + ff'' = 0, \tag{9}$$

$$\left( 1 + \frac{4}{3} k \right) \theta'' + Pr [ f\theta' - f'\theta + E f'^2 ] = 0. \tag{10}$$

Boundary conditions:

$$f(0) = 0, \quad f'(0) = 1, \quad \theta'(0) = 1$$

$$f' \rightarrow 0, \quad \theta \rightarrow 0 \quad \text{as } \eta \rightarrow \infty \tag{11}$$

Where,  $Pr$ ,  $E$ , and  $K$  are the Prandtl, Eckert and radiation numbers respectively.

### 3. Results and discussion

Equations (9) and (10) are solved numerically using the Keller-box method subject to the boundary conditions (11). The method was developed by Keller (1971) and is described in Cebeci and Bradshaw (1977, 1988). From the results, it is seen that variations in Prandtl number  $Pr$ , radiation number  $K$  and Eckert number  $E$  do not affect the value of the wall skin friction coefficient due to the decoupled equations, numerical computation has been carried out to calculate the velocity profiles, temperature profiles, skin friction coefficient and local Nusselt number for various values of the parameters that describe the flow characteristics, i.e., magnetic parameter ( $M$ ), Casson Parameter ( $\gamma$ ), and Porosity parameter ( $K$ ).

**Table 1:** values of the heat transfer coefficient,  $-\theta'(0)$  for various values of  $K$  and  $E$  with  $Pr=1, 2, 3$

K	E=0			E=0.2			E=0.5		
	Pr=1	Pr=2	Pr=3	Pr=1	Pr=2	Pr=3	Pr=1	Pr=2	Pr=3
0	0.9548	1.4714	1.8691	0.8622	1.3055	1.6882	0.5385	0.7248	0.8301
0.3	0.6235	0.9542	0.2542	1.2545	1.0212	0.2154	0.2145	1.0214	1.0214
1	0.5315	0.8627	1.1214	0.4877	0.7818	1.0067	0.3343	0.4984	0.6055

**Table 2:** Values of the heat transfer coefficient,  $-\theta'(0)$  for various values of  $Pr$  and  $E$  with  $K=0, 0.3, 1$

Pr	E=0			E=0.2			E=0.5		
	k=0	K=0.3	K=1	K=0	K=0.3	K=1	K=0	K=0.3	K=1
1	0.2544	0.2555	0.2148	1.2545	1.2154	1.0255	0.1254	1.0244	1.0244
2	1.0241	0.2145	1.0244	1.2542	0.9875	1.2545	1.2544	0.2155	0.2548
3	1.5484	1.2587	1.2548	0.2577	1.0288	1.0254	1.8579	0.2587	1.0879

**Table 3:** values of the heat transfer coefficient,  $-\theta'(0)$  for various values of Pr and K with E=0, 0.2, 0.5

Pr	E=0			E=0.2			E=0.5		
	k=0	K=0.5	K=0.9	K=0	K=0.5	K=0.9	K=0	K=0.5	K=0.9
1	0.9544	1.2555	0.2148	0.2541	0.2154	1.2555	1.1254	1.1544	0.2581
2	0.0641	1.2145	0.0243	0.2541	0.6875	0.2355	1.2122	0.2158	1.2582
3	0.3484	1.2587	0.2541	1.2573	1.0288	1.0125	0.8522	0.1258	1.0258

The numerical results are shown graphically in (Figures 1-9). The comparison of the shown current results corresponding to the values of the Skin friction coefficient,  $f'(0)$  for various values of M in order to know the accuracy of the applied numerical scheme when Prandtl number Pr = 6.2 is made with the available results of Hamad (2011) and presented in Table 1. It is observed that as M increases, the skin friction coefficient also increases. This is due to the fact that an increase in M results in an increase in Lorentz force which opposes the motion of flow. A comparison of the numerical results of the local Nusselt number  $\theta'(0)$  is also done with Vajravelu [54] for various values of the Prandtl number Pr and presented in Table 2. It is clear from Table 2 that the heat transfer rate coefficient increases with an increase in Prandtl number, which is the ratio of momentum diffusivity to thermal diffusivity. So, as Prandtl number increases, the momentum diffusivity increases whereas the thermal diffusivity decreases. Hence, the rate of heat transfer at the surface increases with increasing values of Pr. The results are found to be in excellent agreement. Figure 1 shows the effects of Casson parameter ( $\gamma$ ) on the velocity profile  $f'(\eta)$ , that is  $f'(\eta)$ , is a decreasing function of  $\gamma$ . The momentum boundary layer thickness decreases with an increase in  $\gamma$ , because as the Casson parameter  $\gamma$  increases, the yield stress decreases and as a result the velocity of the fluid is suppressed and the reverse can be seen in Figure 2, which shows the effects of Casson parameter  $\gamma$  on the temperature profile  $\theta(\eta)$ . It can be seen that the temperature of the nanofluids is enhanced with the increasing values of  $\gamma$  and hence the thermal boundary layer thickness increases as the elasticity stress parameter is increased. Figure 3 illustrates the effects of magnetic parameter M on the velocity distribution. From the figure, we can observe that as 'M' increases, the fluid velocity decreases. This is because Lorentz force is induced by the transverse magnetic field and it opposes the motion of the fluid.

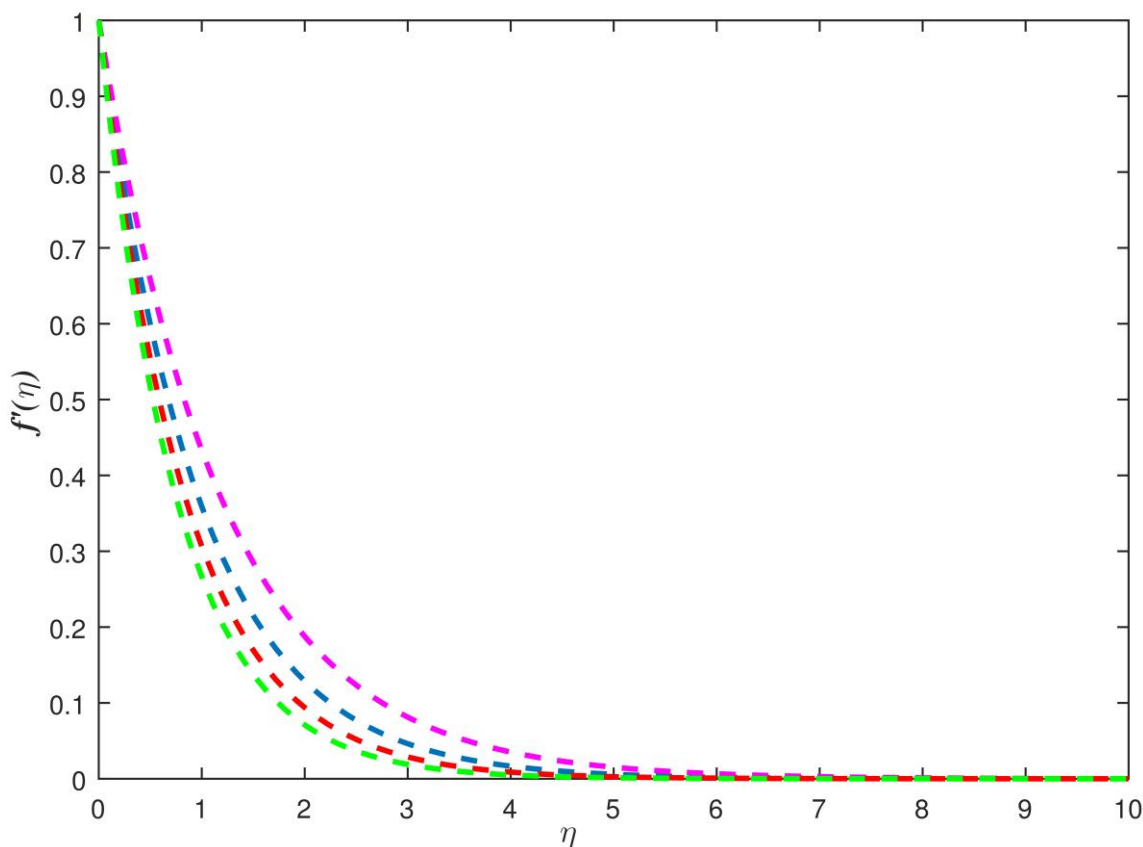


**Figure 1.**

Velocity profiles  $f'(\eta)$  for various values of  $\gamma$  with M=1, k=0.5, Pr= 6.2

For further observation, the effects of E and K with fixed Pr = 1 can be found in Fig. 5. It is shown that as E and K increase, the temperature profiles also increase and the effects of K are more pronounced than the effects of E. On the other hand,

the effects of  $E$  and  $Pr$ , with fixed  $K = 1$ , are illustrated in Fig. 6. It is shown that their effects are the opposite, in which the increase in  $E$  and the decrease in  $Pr$  lead to the increase in the temperature profiles. Finally, the effects of  $K$  and  $Pr$  with fixed  $E = 0.5$  are displayed in Fig. 7. It is shown again that although both  $K$  and  $E$  have the same effects on the temperature profiles, in contrast to the effects of  $Pr$ , the effects of  $K$  are more pronounced than the effects of  $E$ .

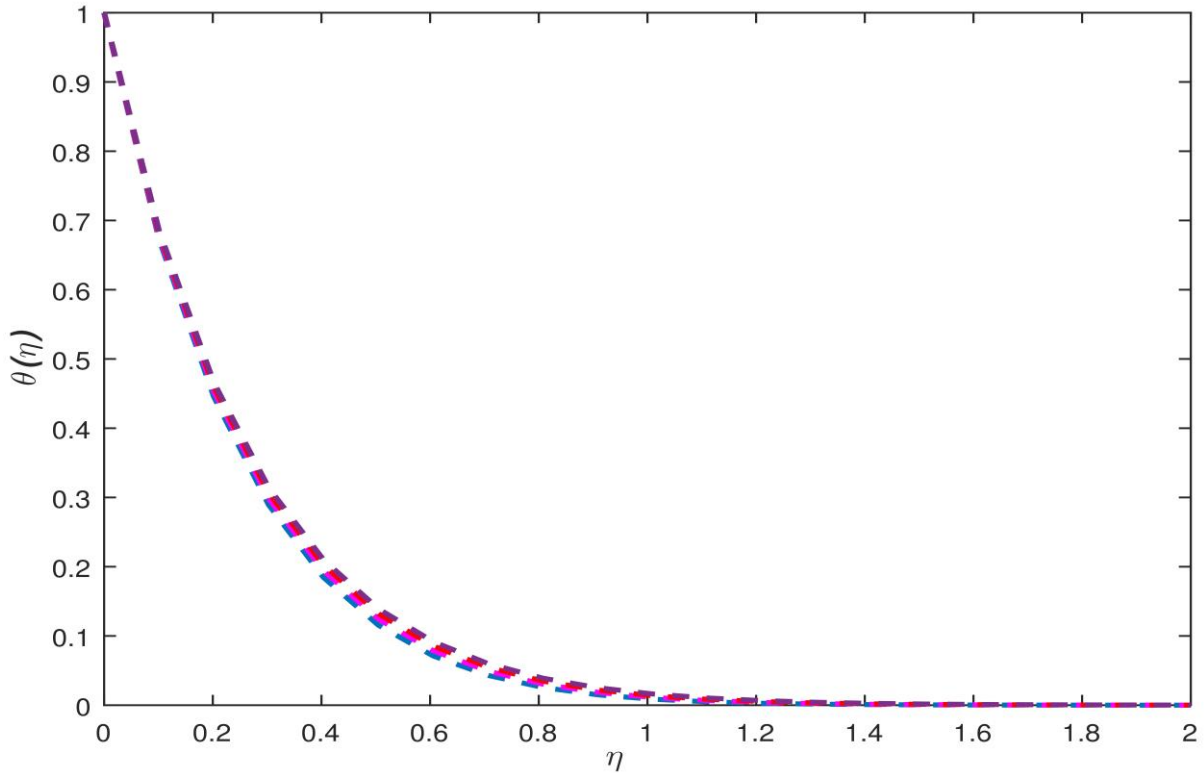


**Figure 2.**

Temperature profiles  $\theta(\eta)$  for various values of  $\gamma=0.5, 1, 2, 5$  with  $M=1; k=0.5; Pr=6.2$

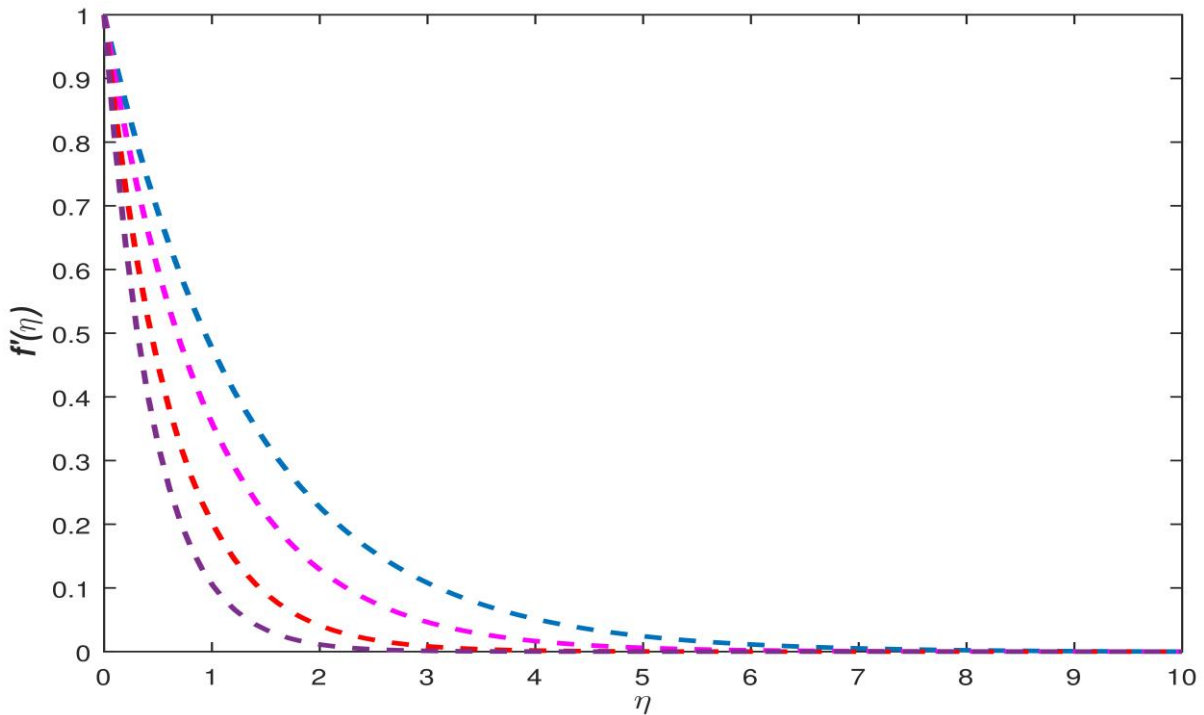


**Figure 3.**

Velocity profiles  $f'(\eta)$  for various values of  $M=0, 1, 2, 3$  for  $\gamma = 1; k=0.5; Pr=6.2$

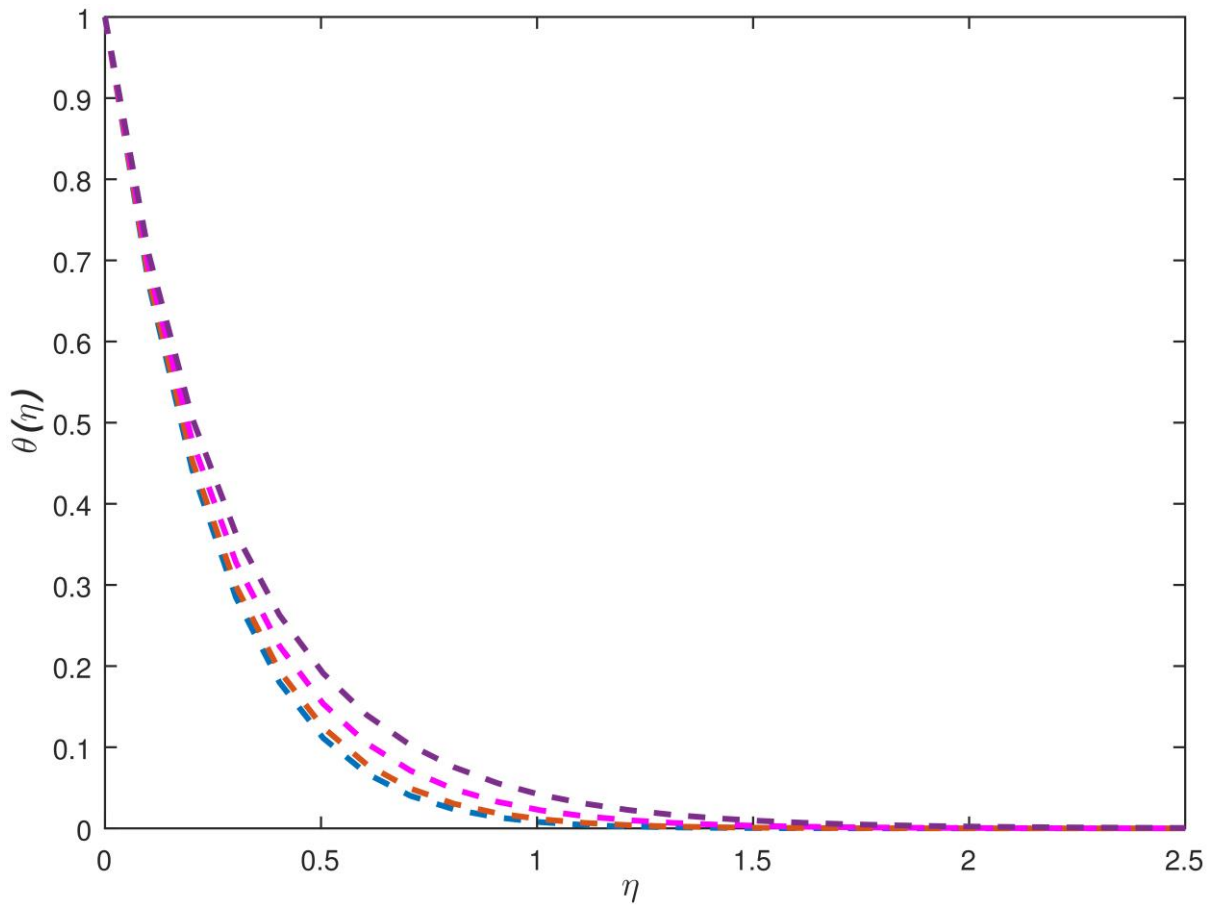


Figure 4.

Temperature profiles  $\theta(\eta)$  for various values of  $M=0, 1, 2, 3$  for  $\gamma = 1; k=0.5; Pr=6.2$

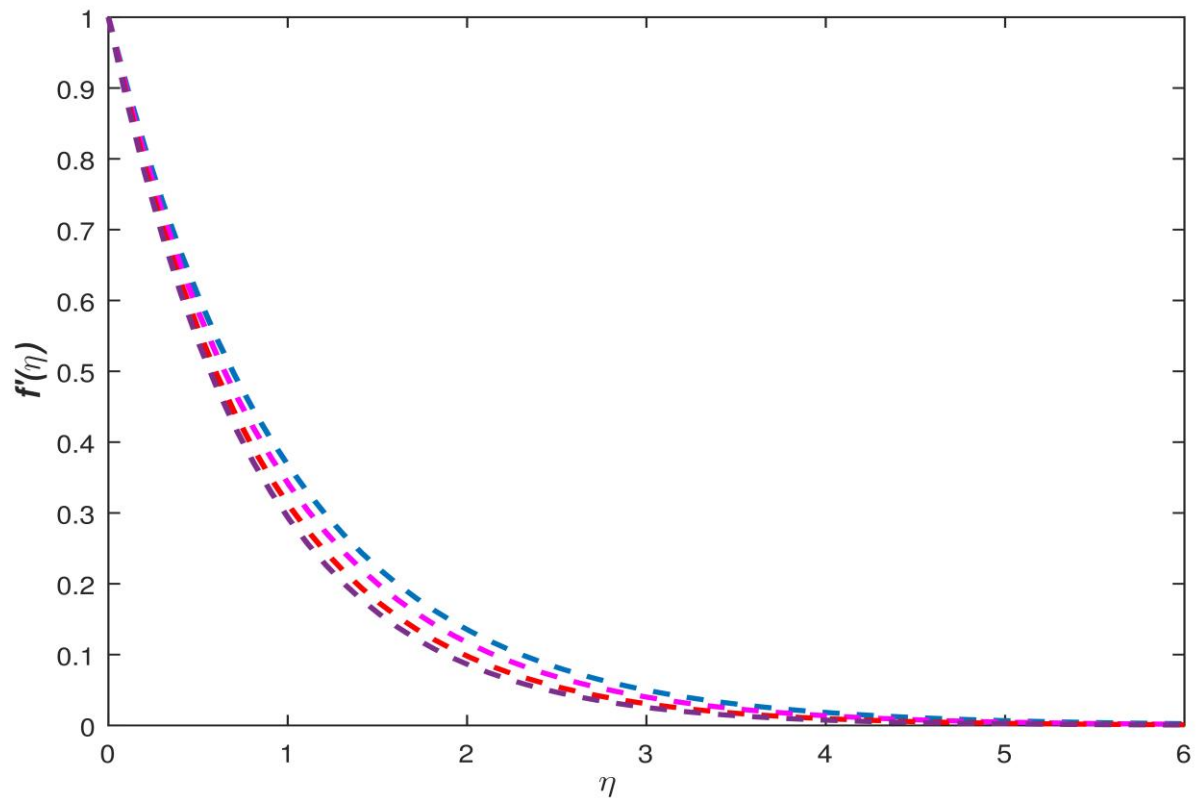


Figure 5.

Velocity profiles  $f'(\eta)$  for various values of  $k = 0, 0.3, 0.7, 1$  for  $\gamma = 1; M=1; Pr=6.2$

MHD flow and heat transfer of Casson nanofluid through a porous medium over a stretching sheet have been investigated. The governing boundary layer equations are transformed into ordinary differential equations using similarity transformations and are then solved by the Keller box method. The effects of the various governing parameters viz. magnetic parameter  $M$ , Casson parameter  $\gamma$ , porosity parameter  $k$  and the nanoparticle volume fraction  $\phi$  on the flow and heat transfer characteristics of two types of nanofluids. The present chapter leads to the following observations:

1. An increase in the Casson parameter  $\gamma$  suppresses the velocity field of the nanofluids whereas the temperature is enhanced.
2. With an increase in the magnetic parameter  $M$ , the momentum boundary layer thickness decreases while the thermal boundary layer thickness increases.
3. The temperature and the thermal boundary thickness increase as the nanoparticle volume fraction  $\phi$  increases.
4. The velocity of the nanofluids decreases as the porosity parameter  $k$  increases and the reverse is observed in the case of temperature.
5. The rate of heat transfer at the surface of the sheet decreases with an increase in magnetic parameter  $M$  and porosity parameter  $k$ .

## References

- [1] Ahmad A, Asghar S (2011) Flow of a second grade fluid over a sheet stretching with arbitrary velocities subject to a transverse magnetic field. *Appl Math Lett* 24:1905–1909
- [2] Bhattacharyya K, Layek GC (2011) Slip effect on diffusion of chemically reactive species in boundary layer flow over a vertical stretching sheet with suction or blowing. *Chem Eng Commun* 198:1354–1365
- [3] Cebeci, T. & Bradshaw, P. 1977. *Momentum transfer in boundary layers*. New York: Hemisphere Publishing Corporation.
- [4] Cebeci, T. & Bradshaw, P. 1988. *Physical and computational aspects of convective heat transfer*. New York: Springer-Verlag.
- [5] Cortell, R. 2008. Radiation effects in the Blasius flow. *Applied Mathematics and Computation* 198: 333-338.
- [6] Domairry G, Ziabakhsh Z (2012) Solution of boundary layer flow and heat transfer of an electrically conducting micropolar fluid in a non-Darcian porous medium. *Meccanica* 47:195–202
- [7] El-Aziz, M.A. 2009. Radiation effect on the flow and heat transfer over an unsteady stretching sheet. *International Communications in Heat and Mass Transfer* 36: 521-524.
- [8] Elbashbeshy, E.M.A. & Dimian, M.F. 2002. Effect of radiation on the flow and heat transfer over a wedge with variable viscosity. *Applied Mathematics and Computation* 132: 445- 454.
- [9] Eldabe NTM, Salwa MGE (1995) Heat transfer of MHD non-Newtonian Casson fluid flow between two rotating cylinders. *J Phys Soc Jpn* 64:41–64
- [10] Fang T, Zhang J, Yao S (2010) A new family of unsteady boundary layers over a stretching surface. *Appl Math Comput* 217:3747–3755
- [11] Hamad MAA(2011) Analytical solution of natural convection flow of a nanofluid over a linearly stretching sheet in the presence of magnetic field. *International Communications in Heat and Mass Transfer* 38:487-492
- [11] Hayat T, Qasim M (2010) Influence of thermal radiation and Joule heating on MHD flow of a Maxwell fluid in the presence of thermophoresis. *Int J Heat Mass Transf* 53:4780–4788
- [12] Hayat T, Shehzad SA, Qasim M (2011a) Mixed convection flow of a micropolar fluid with radiation and chemical reaction. *Int J Numer Methods Fluids* 67:1418–1436
- [13] Hayat T, Shehzad SA, Qasim M, Obaidat S (2011b) Steady flow of Maxwell fluid with convective boundary conditions. *Z Naturforsch* 66a:417–422
- [14] Ishak, A. 2009. Radiation effects on the flow and heat transfer over a moving plate in a parallel stream. *Chinese Physics Letters* 26: 034701.
- [15] RashidiMM, Pour SAM, Abbasbandy S (2011) Analytic approximate solutions for heat transfer of a micropolar fluid through a porous medium with radiation. *Commun Nonlinear Sci Numer Simul* 16:1874–1889
- [16] Rashidi MM, Pour SAM (2010) Analytic approximate solutions for unsteady boundary-layer flow and heat transfer due to a stretching sheet by homotopy analysis method. *Nonlinear Anal Model Control* 15:83–95
- [17] Sajid, M. & Hayat, T. 2008. Influence of thermal radiation on the boundary layer flow due to an exponentially stretching sheet. *International Communications in Heat and Mass Transfer* 35: 347-356.
- [18] Sakiadis, B.C. 1961. "Boundary-layer Behavior on Continuous Solid Surfaces: I Boundary Layer Equations for Two Dimensional and Axisymmetric Flow", *AIChE J* 7, pp. 26-28.
- [19] Shehzad SA, Qasim M, Hayat T, Sajid M, Obaidat S (2013) Boundary layer flow of Maxwell fluid with power law heat flux and heat source. *Int J Numer Methods Heat Fluid Flow* 23:1225–1241
- [20] Vajravelu K (2001) Viscous flow over a nonlinearly stretching sheet. *Applied Mathematics and Computation* 124:281-288
- [21] Yao S, Fang T, Zhong Y (2011) Heat transfer of a generalized stretching/shrinking wall problem with convective boundary conditions. *Commun Nonlinear Sci Num Simul* 16:752–760
- [22] Casson MS. Fluid flow and heat transfer over a nonlinearly stretching surface. *Chinese Physics B*. 2013;**22**: 577-585